Influence of steric effects on the kinetics of cyclic-carbonate vegetable oils aminolysis

Andrés Felipe Guzmán Agudelo, Wander y Pérez-Sena, Nasreddine Kebir, Tapio Salmi, Luis Alberto Ríos, Sébastien Leveneur

Influence of steric effects on the kinetics of cyclic-carbonate vegetable oils aminolysis

Andrés Felipe Guzmán Agudelo[2], Wander Y. Pérez-Sena[1,4], Nasreddine Kebir[3], Tapio Salmi[4],

Luis Alberto Ríos[2], Sébastien Leveneur[1]*

[1]Normandie Université LSPC-Laboratoire de Sécurité des Procédés Chimiques, EA4704,

INSA/Université Rouen, BP08, Avenue de l'Université, 76801 Saint-Etienne-du-Rouvray,

France; E-mail: sebastien.leveneur@insa-rouen.fr

[2]Grupo Procesos Químicos Industriales, Universidad de Antioquia UdeA; Calle 70, No.52-21,

Medellín, Colombia.

[3]Normandie Université, INSA de Rouen, PBS UMR 6270 FR 3038 CNRS, INSA de Rouen, 685

Avenue de l'Université, 76801 Saint Etienne du Rouvray, France.

[4]Laboratory of Industrial Chemistry and Reaction Engineering, Johan Gadolin Process

Chemistry Centre, Åbo Akademi University, Biskopsgatan 8, FI-20500 Åbo/Turku, Finland.

ABSTRACT

Polyurethane polymer is more and more famous because of its versatile properties. The current production process requires the use of isocyanate, which is a hazardous chemical. An alternative eco-friendly route of production is the aminolysis reaction between a cyclic-carbonate, from carbonated vegetable oil, and a diamine. Nevertheless, the kinetics of this reaction system is slow, which might be due to steric hindrance. In order to predict and evaluate this steric hindrance, different amines were tested for the aminolysis of carbonated methyl oleate. Four amines were used: n-butylamine, methylbutylamine, ethylbutylamine and dibutylamine. Kinetic models for the aminolysis with each amine were developed. A relationship between structure and reactivity of each substituent was found through the concept of Linear Free Energy Relationships.

1. Introduction

The main industrial application of vegetable oil is for biodiesel production. The other promising valorization route is for polymer production, particularly polyurethanes. The production capacity of polyurethanes has increased these last years to be the 6th most common polymer in 2014 (Orgiles-Calpena et al., 2016). The reason for this success is the versatile properties of these polymers, which can be applied in different fields such as health sector (biomaterials), automotive, ship-building industry, and bedding (Woods, 1990; Stanzione et al., 2016).

In the industrial scale, the production of polyurethane is based on the reaction between a polyol and di-isocyanate. Even if polyols can be produced from vegetable oils (Pardieu et al., 2016; Petrovic et al., 2008; Lligadas, 2013), di-isocyanate is a petroleum-derived product from the reaction between an amine and phosgene, which is highly unstable and toxic (Kreye et al., 2013).

One of the promising Non-isocyanate polyurethanes (NIPUs) route is the reaction between a five-membered cyclic carbonate and a diamine. The five-membered cyclic carbonate can be produced in a green way from epoxidized vegetable oils and carbon dioxide (Fleischer et al., 2013; Bähr and Mülhaupt, 2012; Foltran et al., 2012; Boyer et al., 2010; Bähr et al., 2012; Cai et al., 2019; Cai et al., 2017). NonoTech Industries company has already developed a Non-isocyanate hybrid polyurethane-epoxy formulation, under the trade name of Green Polyurethane™, for different applications such as coatings, composites, compounds, foams and adhesives (Birukov et al., 2018; Figovsky et al., 2015). The formulations are based on the reaction of partially carbonated and epoxidized vegetable oils with an excess of polyamine compounds leading to crosslinked polyhydroxyurethane (PHU) structures. The curing of these materials can be performed at room temperature thanks to the presence of epoxide groups that are very reactive towards amine groups comparing to 5-membered cyclic carbonates (CCs). Indeed, the aminolysis of 5-membered CCs is limited under moderate conditions, with long reaction times, leading to PHUs with lower average

molecular weights, and mechanical properties compared to commercial PUs (Besse et al., 2015; Tomita et al. 2001). Furthermore, this reaction is not regioselective, leading to a mixture of isomers and can lead to side-reactions at high temperatures (Maisonneuve et al., 2015). Although this reaction is thoroughly studied in the literature and represents the most straightforward pathway to large scale application, realistic solutions to increase reactivity and conversion are still missing because of a lack of kinetics and thermodynamic studies.

In a recent paper of our group, a kinetic model was developed for the aminolysis of carbonated vegetable oils with n-butylamine (Pérez-Sena et al., 2018). However, this model did not consider the steric hindrance of monomers that can seriously affect the reaction kinetics. There is a need to evaluate the steric hindrance for different reactant sizes and to find a general relationship.

The concept of Linear Free Energy Relationships (LFER) can aid in establishing such relationships. This concept has been applied to different systems such as esterification (Lilja et al., 2002), carboxylic acid perhydrolysis (Leveneur et al., 2009), epoxidation (Leveneur, 2017) or hydrogenation of levulinic acid or alkyl levulinates (Wang et al., 2019). In this concept, there is a relationship between the logarithm of the rate constant for one reaction series to polar and steric effects.

The goal of this work was to study the steric effect of amine on the aminolysis of carbonated methyl oleate. For that purpose, kinetic models for aminolysis by butylamine (BA), methylbutylamine (MBA), ethylbutylamine (EBA) and dibutylamine (DBA) were developed. A linear free energy relationship was derived to express the relationship between the amine substituents and their reactivity towards aminolysis.

2. Material and methods

2.1 Materials

The following chemicals were used: formic acid (purity > 98wt%), hydrogen peroxide (purity $\geqslant$ 33wt%), methanol (purity $\geqslant$ 99wt%), and oleic acid (purity $\geqslant$ 82wt%) were purchased from VWR Chemicals. Sulfuric acid (purity $\geqslant$ 95wt%) was from AppliChem. Magnesium sulfate (purity $\geqslant$ 99.5wt%) was from Sigma Aldrich. Tetrabutylammonium bromide (TBAB) and n-butylamine (purity $\geqslant$ 99.5wt%) were purchased from Alfa Aesar.

2.2 Analytical methods

At the esterification step, the acid value was measured according to the standard ASTM D1980 (ASTM, 1998). In the epoxidation and carbonation steps, iodine value was measured according to the standard ASTM D 5554 (ASTM, 2006), and the oxirane oxygen content was measured according to the standard ASTM D 1652-04 (ASTM, 2004). In the aminolysis step, the concentration of carbonate and ester groups was followed through FTIR calibration curves. For preparing the carbonate calibration curve, samples at different times were taken from a typical carbonation reaction. For each sample, the oxirane value was measured, and the difference between the initial and final oxirane values allows knowing the carbonate concentration. Then for each sample, an FTIR run was taken, and the absorbance for carbonate group at 1800 cm^{-1} and a reference group like –CH vibration at 2920 cm^{-1} were measured. The calibration curve was obtained from a linear regression of the arranged data: ratio carbonate absorbance/-CH absorbance vs. concentration of the carbonate group. For preparing the ester calibration curve, different mixes of oleic acid (OA) and methyl oleate (MO) were prepared. With the known masses and average molecular weights of OA and MO, it is possible to calculate the concentration of each sample. Then for each sample, an FTIR run was taken, and the absorbances for the ester group at 1750 cm^{-1} and a reference group like –CH vibration at 2920 cm^{-1} were measured. The calibration curve was

obtained from a linear regression of the arranged data: ratio ester absorbance/-CH absorbance vs. concentration of ester group.

2.3 Production of intermediates

2.3.1 Esterification

The esterification was performed in a lab-scale reactor of 500 mL with mechanical agitation, heating glass jacket and reflux condenser, based on a well-known procedure (Pérez-Sena et al., 2018). Oleic acid, methanol (5:1 mol methanol/mol acid groups) and sulfuric acid (1.8% based on the weight of oleic acid) were mixed at a constant temperature of 65 °C for 3 hours at 500 RPM. Then, the mixture was allowed to settle for 15 minutes, and the upper aqueous phase was appropriately discarded. The organic lower phase was washed five times with distilled water, and the remaining water and methanol were removed by vacuum-rotary evaporation. The acid value of the product was measured to estimate and to confirm the conversion of the process.

By using this protocol, the fatty acid conversion was found to be 95%. No side products were detected for this reaction, and the yield of methyl esters was also 95%. The purity of the so-obtained methyl ester was 95.78 wt%.

2.3.2 Epoxidation

The epoxidation was carried out also in a 500 mL lab-scale reactor equipped with mechanical agitation, heating glass jacket and reflux condenser in semi-batch mode. Methyl oleate and formic acid were charged into the reactor and heated to 55 °C and then, the hydrogen peroxide solution was added dropwise with a pump for 1 hour. The mixing proportion of reactants was 1:0.5:4 molar of double bond/formic acid/hydrogen peroxide. The reaction time was 16 hours, and the stirring speed was fixed to 350 RPM. Then, the system was allowed to settle for 15 minutes, and the lower aqueous phase was removed. The upper organic phase was washed six times with distilled water,

and the remaining water was removed by vacuum rotating evaporation. The iodine value and oxirane oxygen content were measured to the final product to estimate the conversion and yield of the process.

By following this protocol, the double bond conversion was around 98 %, and the epoxide selectivity was 74%.

2.3.3 Carbonation

The carbonation process was carried out in a 600 mL autoclave reactor equipped with mechanical stirring and electrical heating. The reactor was charged with epoxidized methyl oleate (EMO), TBABr catalyst (0.05 mol TBABr per mol epoxide group) and 30 bar of CO_2. The reaction was carried out at 120 °C for 8 hours. After that, ethyl acetate was added in a quantity of 50% based on the EMO weight, and the system was washed five times with distilled water. The remaining water was removed using vacuum rotary evaporation. The oxirane oxygen content was measured to the final product to estimate the conversion of the process.

By using this protocol, the epoxide conversion was 80% with a carbonate selectivity of 90%. The final product obtained after the carbonation reaction has the following properties: oxirane number lower than 0.3%, iodine value of 1.56 g I_2/100 g sample, acid value of 7.46 mg KOH/g sample, and the value of hydroxyl number was found to be 47.54 mg KOH/g sample.

2.3.4 Aminolysis

Experiments were conducted in batch mode under isothermal conditions. The reactor was equipped with mechanical agitation, heating glass jacket and reflux condenser. Table 1 shows the experimental matrix for each run with the initial concentration of ester and carbonated groups and amine. At the beginning of any kinetic experiments, there was no amide group or methanol molecule, so at time zero, their concentrations were zero. One should keep in mind that the

selectivity of the double bond to the epoxide group was lower than 100% during the epoxidation stage, and the epoxide conversion and selectivity of epoxide to cyclic carbonate were also lower than 100%. These experimental results explain the fact that the ratio initial ester concentration to the initial carbonated group concentration is ca. 0.5.

A turbine stirrer was used, and the optimum agitation, i.e., avoiding vortex formation, was found to be 500 RPM.

Four amines were tested: n-butylamine (BA), methylbutylamine (MBA), ethylbutylamine (EBA) and dibutylamine (DBA). It was noticed that as the size of the amine substituent increases, one needs to increase the reaction temperature to observe a significant conversion of the carbonated group.

Despite the presence of a reflux condenser, the reaction temperature was lower than the boiling point of the amines to avoid amine evaporation during the reaction.

For experiments carried out with BA and MBA, it was possible to observe significant carbonated group conversions at reaction temperatures lower than their boiling points. However, for kinetic experiments carried out with EBA, at reaction temperatures lower than its boiling point, it was not possible to observe a significant conversion of the carbonated group. For that reason, the reaction temperature was the boiling point of EBA.

For DBA experiments, the heating system used in this study could not stabilize the reaction temperature when it was higher than 413.15K. If the reaction temperature was lower than 403.15K, then one could not observe a significant carbonated group conversion. For these reasons, two reaction temperatures were tested: 403.15 and 413.15K.

Table 1. Experimental matrix for aminolysis experiments.

	Initial concentration mol/L			T (K)
	Ester	Amine (BA)	Carbonated MO	
RUN1	2.87	3.4	1.23	313.78
RUN2	2.74	3.44	1.23	323.79
RUN3	2.75	3.36	1.21	334.07
	Initial concentration mol/L			T (K)
	Ester	Amine (MBA)	Carbonated MO	
RUN4	2.86	2.97	1.75	344.88
RUN5	2.57	2.95	1.7	355.13
RUN6	2.49	2.93	1.7	364.84
	Initial concentration mol/L			T (K)
	Ester	Amine (EBA)	Carbonated MO	
RUN7	2.68	2.8	1.35	382.15
	Initial concentration mol/L			T (K)
	Ester	Amine (DBA)	Carbonated MO	
RUN8	2.19	2.52	1.15	413.15
RUN9	2.22	2.53	1.19	403.15

3. Results and discussion

During the aminolysis process, there are two reactions: aminolysis producing urethane group and amidation leading to amide group. The latter reaction is reversible. As carbonated methyl oleate is used, then methanol is produced with an amide group. For a complete kinetic model, one must consider the reactivity of the two reaction centers, as shown in Fig. 1.
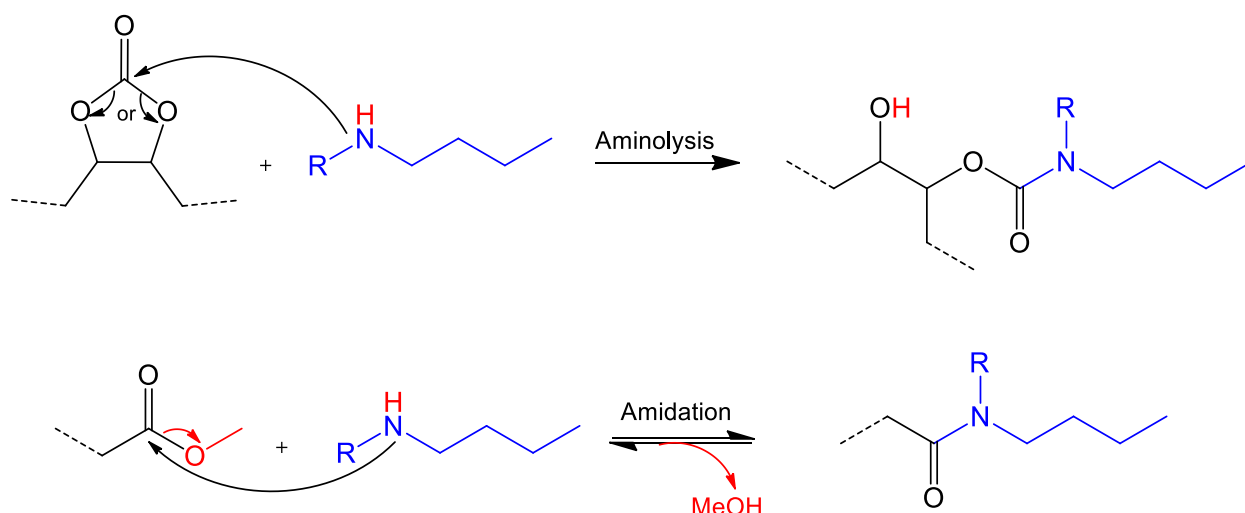

Fig. 1. Reaction scheme for aminolysis and amidation reactions.

As shown in the article by Pérez-Sena et al. (2018), the kinetic expressions for these two reactions can be expressed as:

$$R_{Aminolysis} = k_{Aminolysis} \cdot [Carbonated] \cdot [Amine] \tag{1}$$

$$R_{Amidation} = k_{Amidation} \cdot \left([Ester] \cdot [Amine] - \frac{1}{K_{Amidation}} [Amide] \cdot [Methanol] \right) \tag{2}$$

The amidation equilibrium constant $K_{Amidation}$ was assumed to be temperature-independent for the aminolysis by butylamine and methylbutylamine. Based on the experimental data, the aminolysis of CMO by ethylbutylamine and dibutylamine revealed the amidation reaction was quasi-inexistent. This low reactivity might be linked to thermodynamic limitation.

The material balances for the different compounds in the isothermal batch reactor can be written as

$$\frac{[Carbonated]}{dt} = -R_{Aminolysis} \qquad (3)$$

$$\frac{[Urethane]}{dt} = R_{Aminolysis} \qquad (4)$$

$$\frac{[Amine]}{dt} = -R_{Aminolysis} - R_{Amidation} \qquad (5)$$

$$\frac{[Ester]}{dt} = -R_{Amidation} \qquad (6)$$

$$\frac{[Amide]}{dt} = R_{Amidation} \qquad (7)$$

$$\frac{[Methanol]}{dt} = R_{Amidation} \qquad (8)$$

For kinetic modeling, ModEst software was used (Haario, 2001). The ordinary differential equations (3)-(8) were solved numerically by ODESSA solver implemented in the ModEst software. Non-linear regression was used to estimate the parameters. The concentrations of ester and carbonated groups were used as observables in the regression analysis.

The objective function OF was minimized by the Simplex and Levenberg-Marquardt algorithms,

$$OF = \Sigma\left(C_{i,exp} - C_{i,sim}\right)^2 \qquad (9)$$

where, $C_{i,exp}$ is the experimental concentration, and $C_{i,sim}$ is the concentration simulated by the model.

The coefficient of determination evaluated the reliability of the models to the experimental data,

$$R^2 = 1 - \frac{\Sigma\left(C_{i,exp} - C_{i,sim}\right)^2}{\Sigma\left(C_{i,exp} - \bar{C}_{i,exp}\right)^2} \qquad (10)$$

where, $\bar{C}_{i,exp}$ is the average value of the experimental concentrations.

In the estimation of the kinetic constants the modified Arrhenius equation was used, in order to suppress the natural correlation between the pre-exponential factor and the activation energy,

$$k_R(T) = k_R(T_{Ref}) * \exp\left(\frac{-E_{a_R}}{R}\left(\frac{1}{T} - \frac{1}{T_{Ref}}\right)\right)$$ (11)

where, T_{ref} is a reference temperature.

The standard errors of the parameters were estimated within the confidence interval of 95%.

3.1 Aminolysis of carbonated methyl oleate (CMO) by n-butylamine

Table 2 shows the results of the parameter estimation stage. The estimated results are in the same order of magnitude compared to our previous study (Pérez-Sena et al., 2018). The standard deviation of the estimated constant is low. The coefficient of determination was found to be 99.77%, indicating the reliability of the model.

Table 2. Kinetic constants estimated at Tref=333.15K and statistical data for aminolysis by BA.

	Estimated	Standard deviation %
$k_{Amidation}(T_{Ref})$ (L·mol⁻¹·s⁻¹)	$9.39 \cdot 10^{-06}$	12.90
$Ea_{Amidation}$ (J·mol⁻¹)	45400	16.40
$k_{Aminolysis}(T_{Ref})$ (L·mol⁻¹·s⁻¹)	$6.16 \cdot 10^{-05}$	4.70
$Ea_{Aminolysis}$ (J·mol⁻¹)	42100	7.50
$K_{Amidation}$	$3.03 \cdot 10^{-02}$	16.90

Table S1 shows the correlation matrix of the estimated parameters (See Appendix). One can notice that correlation between the rate constants and their activation energies is quite moderate. For the sake of clarity, only the fit of the model to the experimental data (RUN1) is presented by Fig. 2. The fit of the model for the RUNS 2-3 and the parity plot are in Appendix (Figs S1-S3). One can notice that the fit of the model to the experimental data is very good, which is confirmed by the parity plot, too (Fig. S3).
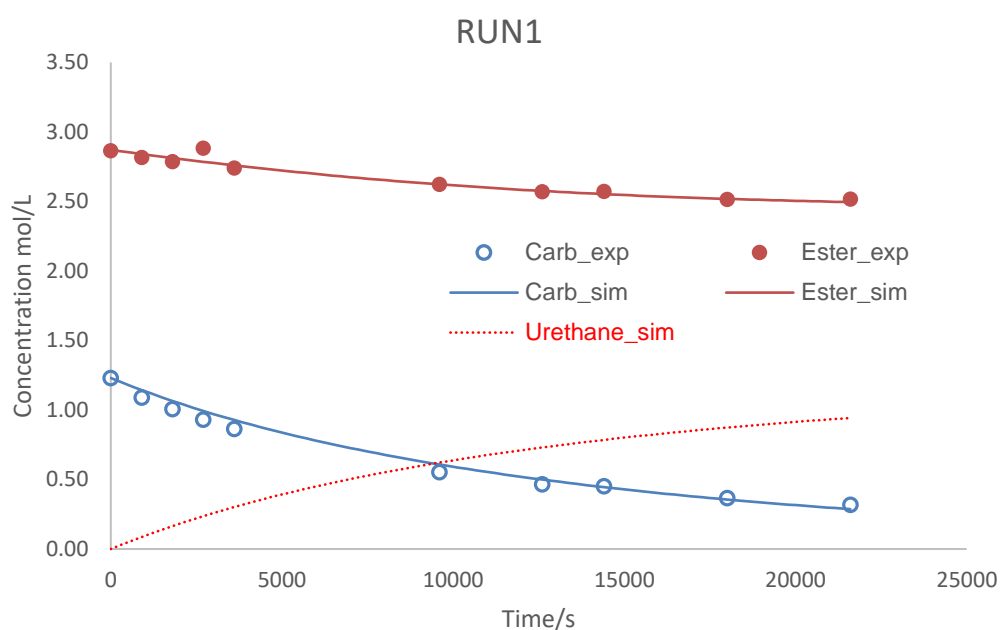

Fig. 2. Fit of the model to the experimental observation for Run 1.

3.2 Aminolysis of carbonated methyl oleate (CMO) by methylbutylamine (MBA)

The estimated parameters with the standard deviations are shown in Table 3. One can notice that the standard deviations are less than 30%, indicating a relatively good estimation of these parameters. The coefficient of determination was calculated to be 99.50%. The correlation between the estimated parameters was very low (Table S2), except between the amidation rate constant at T_{ref} and the equilibrium constant. The moderate correlation between these parameters can be explained by the fact that for this system, the equilibrium constant dependence towards temperature is higher. The model fits perfectly the experimental concentrations (Fig. 3, Figs S4-S6).

Table 3. Kinetic constants estimated at T_{ref}=354.35K and statistical data for aminolysis by MBA.

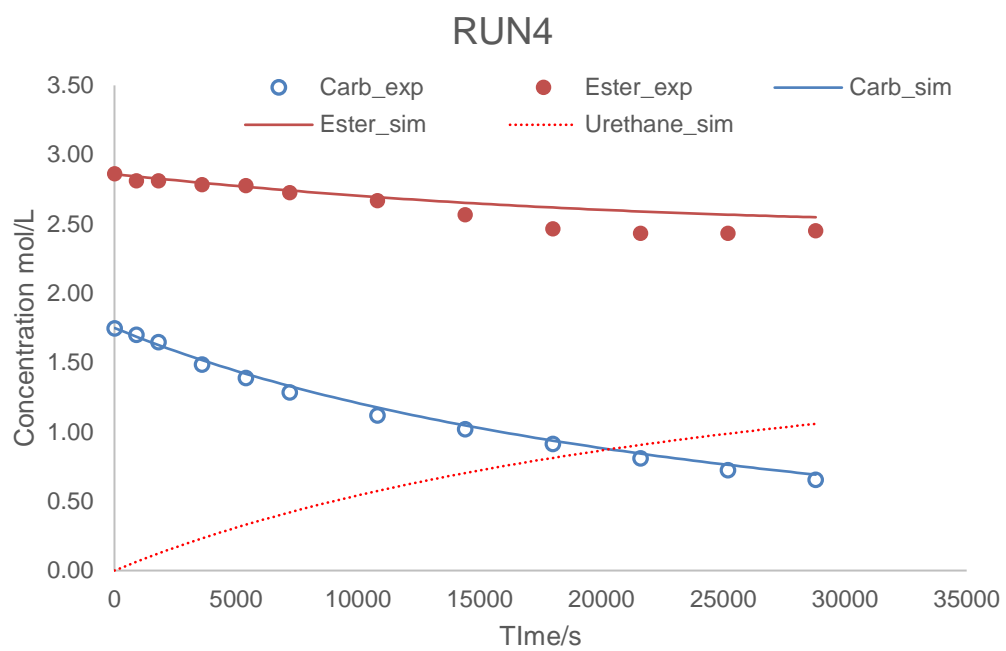|	Estimated	Standard deviation %
$k_{Amidation}\left(T_{Ref}\right)$ (L·mol^{-1}·s^{-1})	$3.16\cdot10^{-06}$	10.20
$Ea_{Amidation}$ (J·mol^{-1})	40000	24.80
$k_{Aminolysis}\left(T_{Ref}\right)$ (L·mol^{-1}·s^{-1})	$2.02\cdot10^{-05}$	2.30
$Ea_{Aminolysis}$ (J·mol^{-1})	40000	7.50
$K_{Amidation}$	$3.50\cdot10^{-02}$	28.30

Fig. 3. Fit of the model to the experimental observation for Run 4.

3.3 Aminolysis of carbonated methyl oleate (CMO) by ethylbutylamine (EBA)

Table 4 shows that the rate constant at 382.15K was estimated to be $2.92 \cdot 10^{-6}$ L.mol^{-1}.s^{-1}. The coefficient of determination was found to be 98.30%. Fig 4 shows the fit of the model to the experimental data. The parity plot figure is displayed in Appendix (Fig. S7).

Table 4. Kinetic constants estimated at T_{ref}=382.15K and statistical data for the aminolysis by EBA.

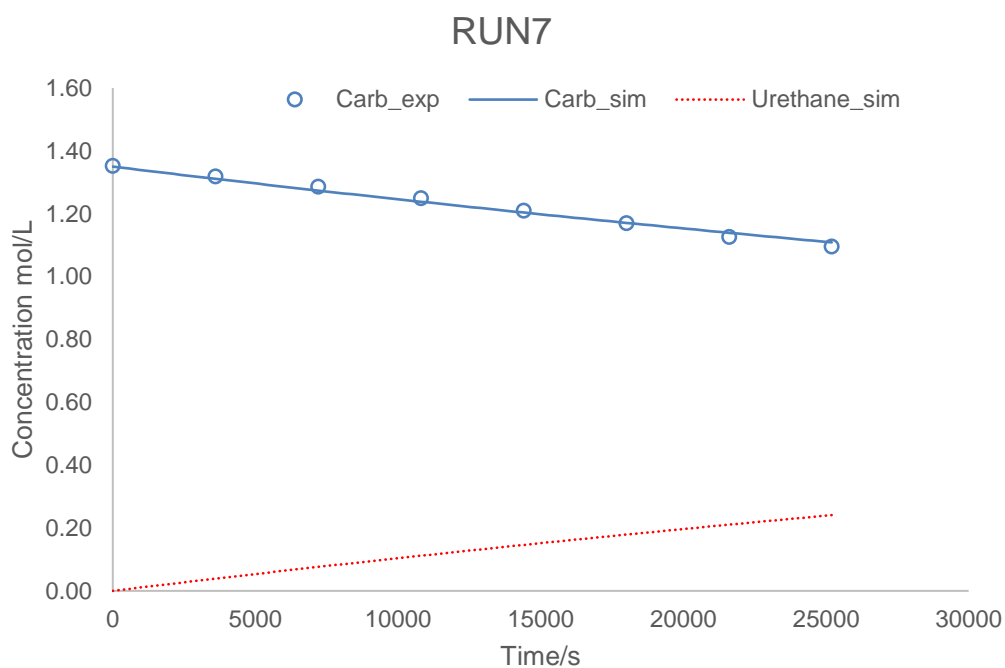|	Estimated	Standard deviation %
$k_{Aminolysis}\left(T_{Ref}\right)$ (L·mol^{-1}·s^{-1})	$2.92 \cdot 10^{-6}$	2.6

Fig. 4. Fit of the model to the experimental observation for Run 7.

3.4 Aminolysis of carbonated methyl oleate (CMO) by dibutylamine (DBA)

Table 5 shows the estimated parameters along with the standard deviations. It can be noticed that the standard deviations are very low, confirming a relatively good estimation of these parameters. The coefficient of determination was calculated to be 99.09%. The correlation between the rate constant and the activation energy was very low, i.e., -0.22. The model fits perfectly the experimental data (Fig 5, Figs S8-S10).

Table 5. Kinetic constants estimated at T_{ref}=408.15K and statistical data for aminolysis by DBA.

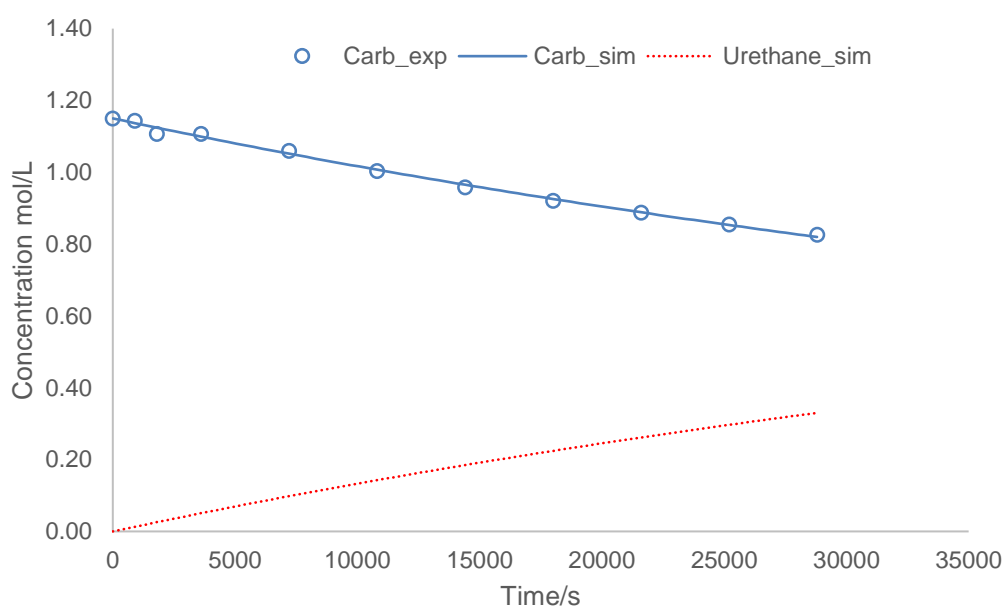|	Estimated	Standard deviation %
$k_{Aminolysis}\left(T_{Ref}\right)$ $(L \cdot mol^{-1} \cdot s^{-1})$	$4.16 \cdot 10^{-06}$	1.60
Ea_Aminolysis $(J \cdot mol^{-1})$	52900.00	8.50

Fig. 5. Fit of the model to the experimental observation for Run 8.

3.5 Comparisons

Fig. 6 shows the evolution of the aminolysis rate constants at different temperatures for BA, MBA and DBA. It can be noticed that the rates of aminolysis increase in the following way: $R_{Aminolysis\ by\ BA} > R_{Aminolysis\ by\ MBA} > R_{Aminolysis\ by\ DBA}$ at any temperatures. At 382.15 K, the rate increases in the following way $R_{Aminolysis\ by\ BA} > R_{Aminolysis\ by\ MBA} > R_{Aminolysis\ by\ EBA} > R_{Aminolysis\ by\ DBA}$. As the steric hindrance substituent increases, the kinetics of aminolysis decreases.
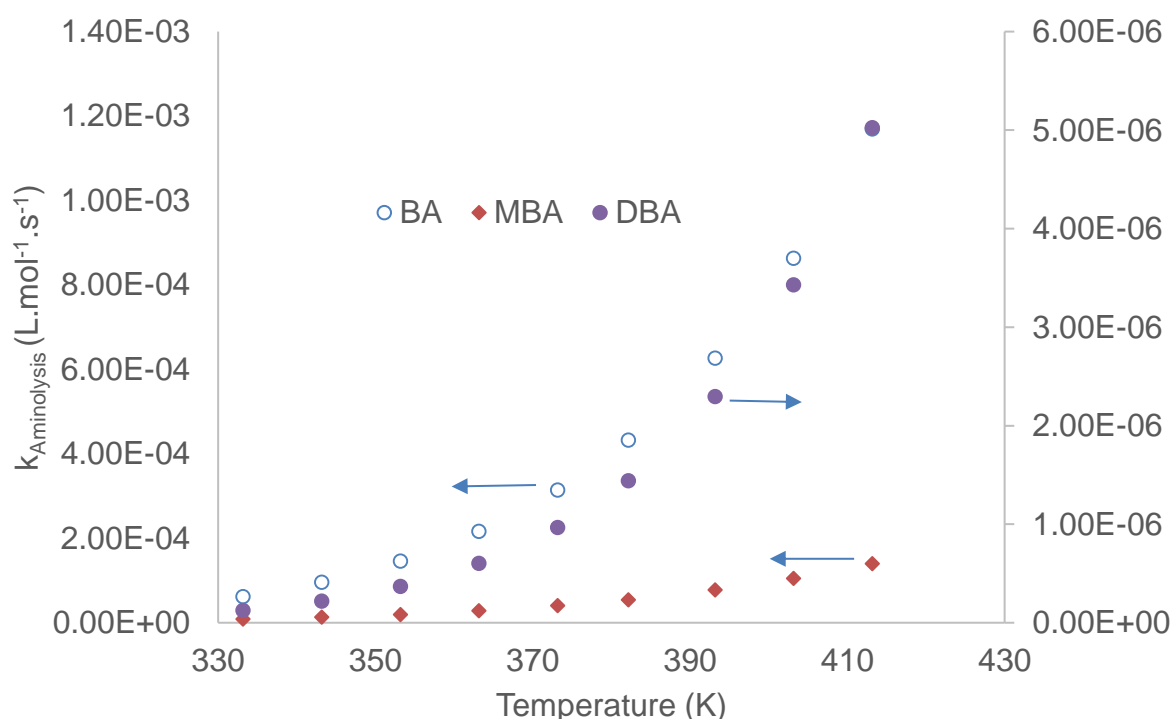

Fig. 6 Evolution of aminolysis rate constants at different temperatures and substituents.

In this study, a linear free energy relationship was used to find a relationship (Eq. 11) between the substituent reactant and kinetics.

$$log(k_X) = a \cdot b_x + c \tag{11}$$

The coefficient b_x depends on the substituents –H (for BA), -Me (for MBA), -Et (for EBA) and –Bu (for DBA). This coefficient represents the total steric effect of the substituent.

Table 6 displays the values of b_x tested in this study. Fig. 7 demonstrates that Eq. (11), using values from Table 6, is correct at different temperatures. A value of 3 for b_x was given for Bu- substituent because it gives the best statistical results. One can notice that the values of a and c are temperature dependent. Fig. 7 shows that Eq. (11) establishes a correlation between reaction rates and substituent for aminolysis reaction.

This study shows that the aminolysis reaction depends on the steric hindrance of amine substituent. By increasing the reaction temperature, the importance of the steric effect on the reaction series, i.e., the absolute values of a and c decrease with the increase of reaction temperature.

Table 6. Values of b_x from Eq. (11).

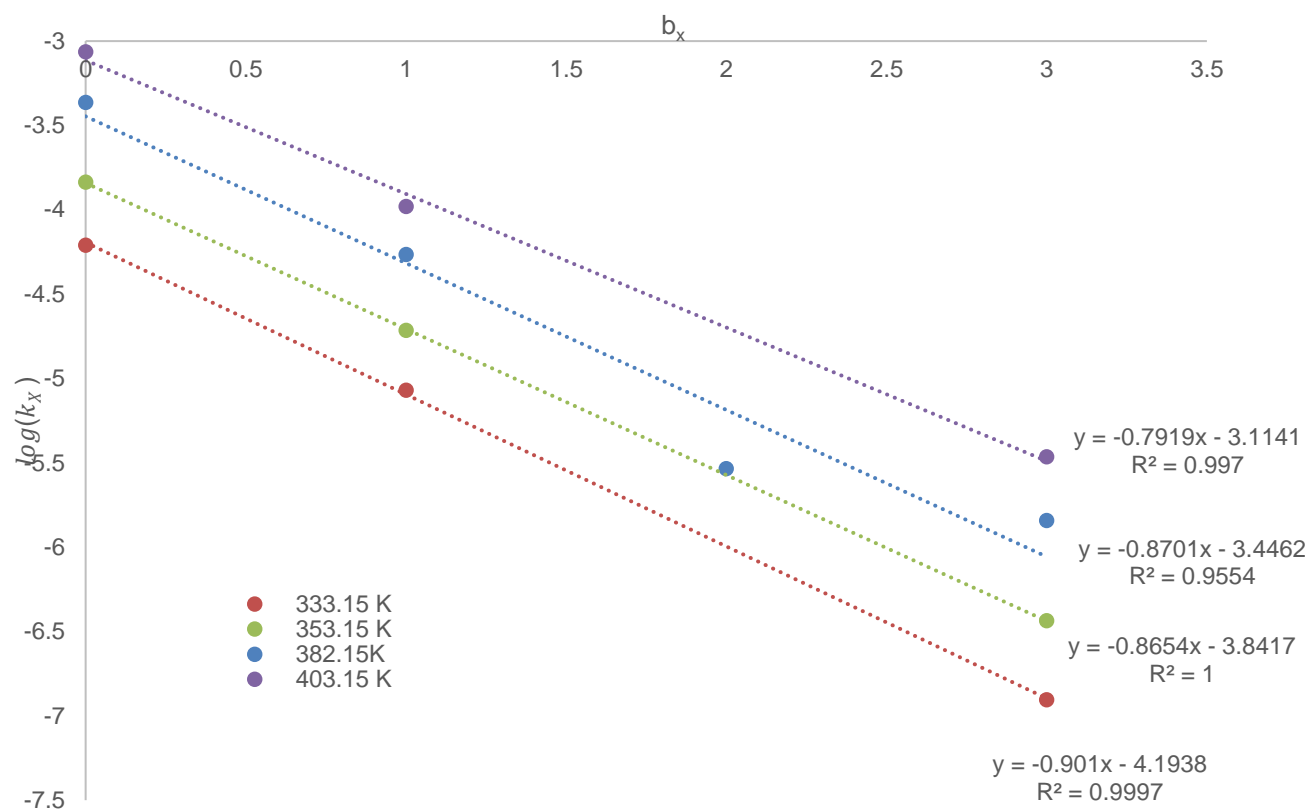| Substituents	b_x
H-	0
Me-	1
Et-	2
Bu-	3

Fig. 7. Application of Eq. (11) to the aminolysis system.

4. Conclusions

A kinetic study for the aminolysis of carbonated methyl oleate by amines with different steric hindrance was performed. Butylamine, methylbutylamine, ethylbutylamine and dibutylamine were screened as reactants.

A direct comparison between the kinetics with these amines is not possible, because the optimum reaction temperature is not the same. Hence, a kinetic model was developed for each aminolysis system, and it was found that as the steric hindrance of amine increases, the rate constant is smaller. It was found that the amidation reaction is negligible for the aminolysis by ethylbutylamine and dibutylamine. As expected, activation energies are quite similar, within 45000-52900 $J \cdot mol^{-1}$, indicating that the decrease in the rate constants is indeed due to the increase in the steric hindrance of the amines that leads to a lower probability of collisions.

A relationship between substituent structure and reactivity was found for the aminolysis reaction by using the concept of the linear free energy relationship. The logarithm of the aminolysis rate constant can be expressed by a linear function with b_x, which measures the steric hindrance of the amine substituent. It was demonstrated that the two other parameters *a* and *c* are temperature dependent.

More investigation on the theoretical interpretation of b_x, *a* and *c* are needed in order to be able to predict the reactivity of different amines for the aminolysis reaction. Such an approach could contribute to finding adequate diamine and optimum operating conditions for the production of Non-isocyanate polyurethane.

Notation

Amide	amide groups
C	concentration
Carbonated	carbonated groups
Ea	activation energy [kJ.mol^{-1}]
FTIR	Fourier transform infrared spectroscopy
^{1}H-NMR	proton nuclear magnetic resonance
k	reaction rate constant or kinetic constant [L.mol^{-1}.s^{-1}]
K_c	equilibrium constant
MeOH	methanol
R	reaction rate [mol.L^{-1}.s^{-1}]
r	reaction rate for a reactant or product [mol.L^{-1}.s^{-1}]
T	temperature [K]
t	time [s]
V	volume [L]

Subscripts and superscripts

0	initial
Amid	amidation
Aminol	aminolysis
i	component i
R	reaction

Abbreviations

BA	butylamine
CMO	carbonated methyl oleate
DBA	dibutylamine
EBA	ethylbutylamine
EMO	epoxidized methyl oleate
MBA	methylbutylamine
MO	methyl oleate
OF	objective function
nBA	n-butylamine
OA	oleic acid
TBABr	tetra-n-butylammonium bromide

Acknowledgments

References

ASTM D1980, 1998. Standard Test Method for Acid Value of Fatty Acids and Polymerized Fatty Acids.

ASTM D 1652-04, 2004. Standard Test Method for Epoxy Content of Epoxy Resins.

ASTM D5554, 2006. Standard Test Method for Determination of the Iodine Value of Fats and Oils.

Bähr, M., Bitto, A., Mülhaupt, R., 2012. Cyclic limonene dicarbonate as a new monomer for non-isocyanate oligo- and polyurethanes (NIPU) based upon terpenes. Green Chem. 14, 1447–1454. https://doi.org/10.1039/C2GC35099H

Bähr, M., Mülhaupt, R., 2012. Linseed and soybean oil-based polyurethanes prepared via the non-isocyanate route and catalytic carbon dioxide conversion. Green Chemistry 14, 483–489. https://doi.org/10.1039/C2GC16230J

Besse, V., Camara, F., Méchin, F., Fleury, E., Caillol, S., Pascault, J.-P., Boutevin, B., 2015. How to explain low molar masses in PolyHydroxyUrethanes (PHUs). European Polymer Journal 71, 1–11. https://doi.org/10.1016/j.eurpolymj.2015.07.020

Birukov, O., Figovsky, O., Leykin, A., Potashnikov, R., Shapovalov, L., 2018. Method of producing hybrid polyhydroxyurethane network on a base of carbonated-epoxidized unsaturated fatty acid triglycerides, CA Patent CA2767784C, February 27.

Boyer, A., Cloutet, E., Tassaing, T., Gadenne, B., Alfos, C., Cramail, H., 2010. Solubility in CO_2 and carbonation studies of epoxidized fatty acid diesters: towards novel precursors for polyurethane synthesis. Green Chem. 12, 2205–2213. https://doi.org/10.1039/C0GC00371A

Cai, X., Matos, M., Leveneur, S., 2019. Structure–Reactivity: Comparison between the Carbonation of Epoxidized Vegetable Oils and the Corresponding Epoxidized Fatty Acid Methyl Ester. Ind. Eng. Chem. Res. 58, 1548–1560. https://doi.org/10.1021/acs.iecr.8b05510

Cai, X., Zheng, J.L., Wärnå, J., Salmi, T., Taouk, B., Leveneur, S., 2017. Influence of gas-liquid mass transfer on kinetic modeling: Carbonation of epoxidized vegetable oils. Chemical Engineering Journal 313, 1168–1183. https://doi.org/10.1016/j.cej.2016.11.012

Figovsky, O., Potashnikov, R., Leykin, A., Shapovalov, L., Sivokon, S., 2015. Method for forming a sprayable nonisocyanate polymer foam composition, US Patent US20150024138A1, January 22.

Fleischer, M., Blattmann, H., Mülhaupt, R., 2013. Glycerol-, pentaerythritol- and trimethylolpropane-based polyurethanes and their cellulose carbonate composites prepared via the non-isocyanate route with catalytic carbon dioxide fixation. Green Chem. 15, 934–942. https://doi.org/10.1039/C3GC00078H

Foltran, S., Maisonneuve, L., Cloutet, E., Gadenne, B., Alfos, C., Tassaing, T., Cramail, H., 2012. Solubility in CO_2 and swelling studies by in situ IR spectroscopy of vegetable-based epoxidized oils as polyurethane precursors. Polym. Chem. 3, 525–532. https://doi.org/10.1039/C2PY00476C

Haario, H., 2001. MODEST-User's Guide. Profmath Oy, Helsinki.

Kreye, O., Mutlu, H., Meier, M.A.R., 2013. Sustainable routes to polyurethane precursors. Green Chem. 15, 1431–1455. https://doi.org/10.1039/C3GC40440D

Leveneur, S., 2017. Thermal Safety Assessment through the Concept of Structure–Reactivity: Application to Vegetable Oil Valorization. Org. Process Res. Dev. 21, 543–550. https://doi.org/10.1021/acs.oprd.6b00405

Leveneur, S., Murzin, D.Yu., Salmi, T., 2009. Application of linear free-energy relationships to perhydrolysis of different carboxylic acids over homogeneous and heterogeneous catalysts. Journal of Molecular Catalysis A: Chemical 303, 148–155. https://doi.org/10.1016/j.molcata.2009.01.017

Lilja, J., Murzin, D.Yu., Salmi, T., Aumo, J., Mäki-Arvela, P., Sundell, M., 2002. Esterification of different acids over heterogeneous and homogeneous catalysts and correlation with the Taft equation. Journal of Molecular Catalysis A: Chemical 182–183, 555–563. https://doi.org/10.1016/S1381-1169(01)00495-2

Lligadas, G., 2013. Renewable Polyols for Polyurethane Synthesis via Thiol-ene/yne Couplings of Plant Oils. Macromolecular Chemistry and Physics 214, 415–422. https://doi.org/10.1002/macp.201200582

Maisonneuve, L., Lamarzelle, O., Rix, E., Grau, E., Cramail, H., 2015. Isocyanate-Free Routes to Polyurethanes and Poly(hydroxy Urethane)s. Chem. Rev. 115, 12407–12439. https://doi.org/10.1021/acs.chemrev.5b00355

Orgilés-Calpena, E., Arán-Aís, F., Torró-Palau, A.M., Montiel-Parreño, E., Orgilés-Barceló, C., 2016. Synthesis of polyurethanes from CO2-based polyols: A challenge for sustainable adhesives. International Journal of Adhesion and Adhesives, Special Issue on Adhesion, Surface Preparation and Adhesive Properties 67, 63–68. https://doi.org/10.1016/j.ijadhadh.2015.12.027

Pardieu, E., Chau, N.T.T., Dintzer, T., Romero, T., Favier, D., Roland, T., Edouard, D., Jierry, L., Ritleng, V., 2016. Polydopamine-coated open cell polyurethane foams as an inexpensive, flexible yet robust catalyst support: a proof of concept. Chem. Commun. 52, 4691–4693. https://doi.org/10.1039/C6CC00847J

Pérez-Sena, W.Y., Cai, X., Kebir, N., Vernières-Hassimi, L., Serra, C., Salmi, T., Leveneur, S., 2018. Aminolysis of cyclic-carbonate vegetable oils as a non-isocyanate route for the synthesis of polyurethane: A kinetic and thermal study. Chemical Engineering Journal 346, 271–280. https://doi.org/10.1016/j.cej.2018.04.028

Petrović, Z.S., 2008. Polyurethanes from Vegetable Oils. Polymer Reviews 48, 109–155. https://doi.org/10.1080/15583720701834224

Stanzione, M., Russo, V., Sorrentino, A., Tesser, R., Lavorgna, M., Oliviero, M., Di Serio, M., Iannace, S., Verdolotti, L., 2016. Bio-based polyurethane foams from renewable resources. AIP Conference Proceedings 1736, 020130. https://doi.org/10.1063/1.4949705

Tomita, H., Sanda, F., Endo, T., 2001. Polyaddition behavior of bis(five- and six-membered cyclic carbonate)s with diamine. J. Polym. Sci. Pol. Chem. 39, 860–867. https://doi.org/10.1002/1099-0518(20010315)39:6<860::AID-POLA1059>3.0.CO;2-2

Wang, Y., Cipolletta, M., Vernières-Hassimi, L., Casson-Moreno, V., Leveneur, S., 2019. Application of the concept of Linear Free Energy Relationships to the hydrogenation of levulinic acid and its corresponding esters. Chemical Engineering Journal 374, 822–831. https://doi.org/10.1016/j.cej.2019.05.218

Woods, G., 1990. The ICI Polyurethanes book, 2nd ed., Wiley, New York.